POLITECNICO DI TORINO
Repository ISTITUZIONALE

Optical properties of recent non-fullerene molecular acceptors for bulk heterojunction solar cells

(Article begins on next page)
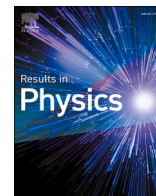
15 January 2025

Optical properties of recent non-fullerene molecular acceptors for bulk heterojunction solar cells

Andrea Farina [a], Giuseppe M. Paternò [b], Francesco Scotognella [b,c,*]

[a] Istituto di Fotonica e Nanotecnologie, Consiglio Nazionale delle Ricerche, Piazza Leonardo da Vinci 32, 20133 Milano, Italy
[b] Center for Nano Science and Technology@PoliMi, Istituto Italiano di Tecnologia, Via Pascoli 70/3, 20133 Milano, Italy
[c] Dipartimento di Fisica, Politecnico di Milano, Piazza Leonardo da Vinci 32, 20133 Milano, Italy

ABSTRACT

For many years the faith of organic photovoltaics has been linked to the one of fullerene, since fullerene has been considered the electron-acceptor of choice in bulk heterojunctions solar cells. In the last years, the number of molecules that can be very competitive in replacing fullerene has increased significantly. In this work, we study by means of different theoretical methods five molecules that have demonstrated to work effectively as acceptors in organic heterojunctions. We discuss the comparison of simulated absorption spectra with the experimental spectra.

Introduction

In the last decades, fullerene-based materials have been the most used acceptors in organic bulk heterojunction solar cells, owing to their relatively high processability and to the delocalization of the lowest unoccupied molecular orbital (LUMO) across the entire three-dimensional surface of fullerene [1]. Since the first report on the use of polymer:fullerene heterojunction as photovoltaic material in 1992 [2], the use of fullerene derivatives has seen a stark increase [3–9]. On the other hand, some intrinsic limitations of fullerenes, such the generally weak optical absorption in the visible and its environmental instability [10], have promoted the research of new non-fullerene acceptors [11]. The outstanding endeavour in chasing reliable substitutes to fullerene is, for example, testified by works on perylenediimide-based molecules [12] and on fluorene-based molecules [13], and reported in four exhaustive review articles published in 2017 [14] and 2019 [11,15,16]. Remarkably, power conversion efficiencies (PCE) above 16% have been achieved for solar cells integrating the non-fullerene acceptor BTPTT-4F [17–19]. In this context, also semiconducting carbon nanotubes have been proposed as valid alternative to fullerenes, due to their excitonic behaviour and relatively high environmental stability [20–22].

In this work, we simulate by employing different calculation methods the absorption properties of non-fullerene molecules that hold great promises as efficient electron- acceptor systems in organic heterojunction solar cells. The study of the optical gap and of the different optical transitions in non-fullerene acceptors permit to corroborate and complement the experimental studies present in the literature and aims at a better understanding of the different electronic transitions in the studied molecules.

Methods

We have sketched the molecule geometries with the Avogadro package [23]. We have optimized the ground state geometries and we have calculated the electronic transitions of the molecules with the package ORCA 4.2.1 [24].

Density Functional Theory calculations (with B3LYP functional): We have used the B3LYP functional [25] in the framework of the density functional theory. We have employed the Ahlrichs split valence basis set [26] and the all-electron nonrelativistic basis set SVPalls1 [27,28]. Moreover, the calculation utilizes the Libint library [29] and the Libxc library [30,31].

Density Functional Theory calculations (with BP functional): We employ ORCA 4.2.1 [24] for these calculations. The orbital basis set def2-SVP has been used [32] and the auxiliary basis set def2/J has been used [33]. Also in this case, the calculation utilizes the Libint library [29] and the Libxc library [30,31].

Calculations with Zerner's Intermediate Neglect of Differential Overlap (ZINDO/S), Modified Neglect of Diatomic Overlap (MNDO), Parametric Method 3 (PM3) methods: Also for these calculations we employ ORCA 4.2.1 [24]. The orbital basis set def2-SVP has been used [32]. Also in this
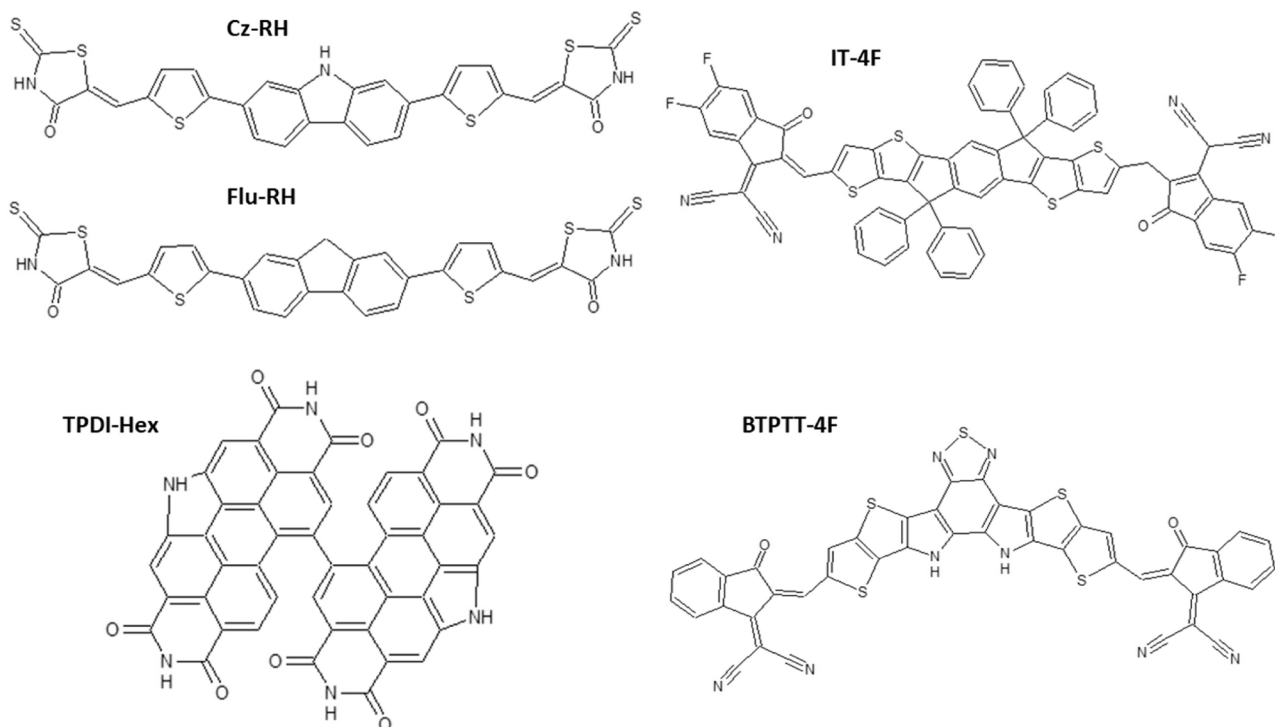
* Corresponding author.

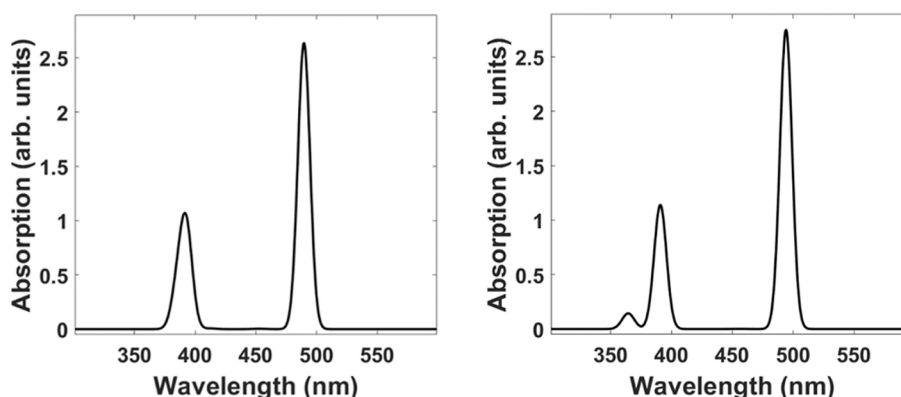**Fig. 1.** Molecular structures of the molecules studied: Cz-RH, Flu-RH, TPDI-Hex, IT-4F and BTPTT-4F.

Fig. 2. Calculation of the absorption spectrum (DFT with B3LYP functional) of the molecule Cz-RH (left) and the molecule Flu-RH (right).

case, the calculation utilizes the Libint library [29] and the Libxc library [30,31].

Calculations with Hückel method: For the Hückel we employ the Hulis package [34,35].

Results and discussion

In Fig. 1, we show the molecular structures of the five investigated molecules. The molecule with 3-ethylrhodanine (RH) attached to both ends of thiophene-flanked carbazole is the so-called Cz-RH [36]. A solar cell that includes a bulk heterojunction with Poly(3-hexylthiophene) and Cz-RH (P3HT-Cz-RH) is reported in literature with a power conversion efficiency (PCE) of 2.56% [37].

The N-annulated perylene diimide (PDI) dimer has been employed in a bulk heterojunction solar cell reaching power conversion efficiency up to 7.6% with a terthiophene-based polymer named P3TEA as donor material [38]. The molecule IT-4F is used as acceptor in a bulk heterojunction with fluorinated poly[(2,6-(4,8-bis(5-(2-ethylhexyl)thiophen-2-yl)benzo[1,2-b:4,5-b′]dithiophene)-*co*-(1,3-di(5-thiophene-2-yl)-5,7-

bis(2-ethylhexyl)benzo[1,2-c:4,5-c′]dithiophene-4,8-dione)] (PBDB-T-SF) leads to a PCE of 13% [39,40]. Finally, a heterojunction containing BTPTT-4F shows an efficiency above 16% as mentioned above [17].

We have calculated the first 16 transitions for the studied molecules (reported in the Supporting Information) and obtained simulated absorption spectra as a sum of Gaussian curves expressed as $f(x) = f_{osc}\exp\left[(x - x_c)^2/2a^2\right]$, with f_{osc} the oscillator strength of the transition, x_c the central wavelength (in nm) of the transition, a that is related to the linewidth. In particular, we have selected a value of 5 nm for the linewidth a. In Fig. 2, we show the simulations of the absorption spectra of Cz-RH molecule (left) and Flu-RH molecule (right). The lowest transition peak at around 500 nm (about 2.48 eV) is in good agreement with the experimental absorption spectra for the solutions reported in Kim at *al.* [37]. The highest predicted transitions are at longer wavelengths with respect to the experimental ones.

In Fig. 3, we show the absorption spectrum of TPDI-Hex. We observe a discrepancy between the simulated absorption spectrum and the experimental one in terms of oscillator strength. The lowest simulated
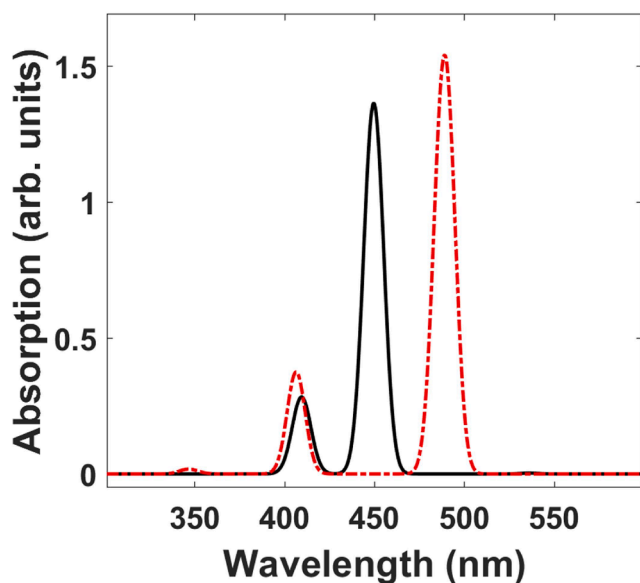
Fig. 3. Calculation of the absorption spectrum of TPDI-Hex with DFT and B3LYP functional (solid black curve) and ZINDO/S method (dotted dashed red curve). (For interpretation of the references to colour in this figure legend, the reader is referred to the web version of this article.)
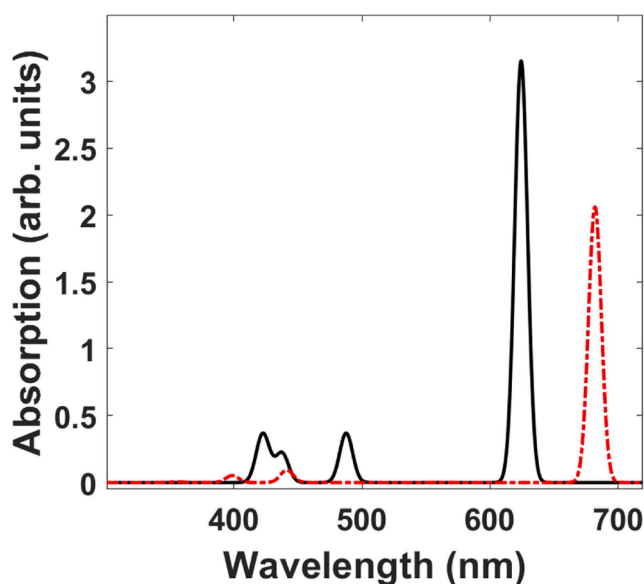
Fig. 4. Calculation of the absorption spectrum of IT-4F with DFT and B3LYP functional (solid black curve) and with ZINDO/S method (dotted dashed red curve). (For interpretation of the references to colour in this figure legend, the reader is referred to the web version of this article.)

transition is at 2.31 eV (with a very weak oscillator strength of < 0.01) while the lowest experimental transition is at 2.36 eV, but with a very strong weight in the spectrum with respect to the other peaks. With ZINDO/S method the simulated lowest transition is at 2.52 eV (with an oscillator strength of 0.93). These discrepancies could be due to the optimized geometry used and, in particular, to the dihedral angle between the perylene groups.

In Fig. 4, we show the absorption spectrum of IT-4F with the lowest optical transition at 1.99 eV with DFT and B3LYP functional (black solid curve) and at 1.82 eV with ZINDO/S, while the experimental absorption shows the lowest absorption peak at 1.77 eV [39,40].

In Fig. 5, we display the absorption spectrum of BTPTT-4F, with the

Fig. 5. Calculation of the absorption spectrum of BTPTT-4F with DFT and B3LYP functional (solid black curve) and with ZINDO/S method (dotted dashed red curve). (For interpretation of the references to colour in this figure legend, the reader is referred to the web version of this article.)
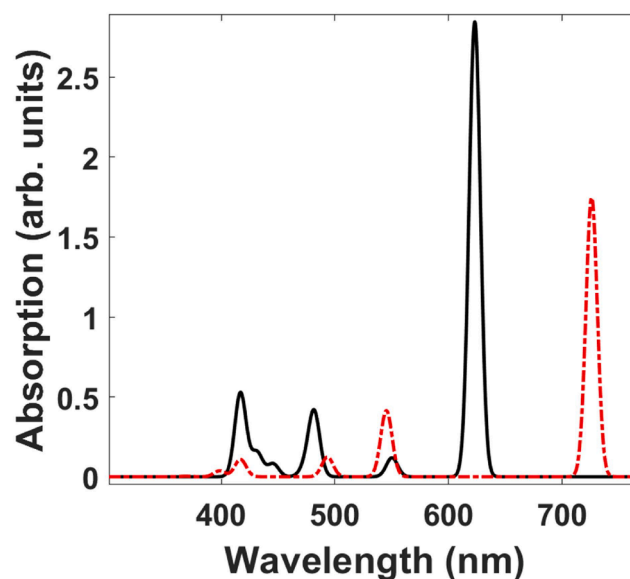
Table 1
Optical band gap of BTPTT-4F calculated with different methods: DFT with B3LYP and BP functional, Zerner's Intermediate Neglect of Differential Overlap (ZINDO/S), Modified Neglect of Diatomic Overlap (MNDO), Parametric Method 3 (PM3).

	DFT B3LYP	DFT BP	ZINDO/S	MNDO	PM3
Optical band gap (eV)	1.99	1.65	1.71	2.01	2.28

transition at 1.99 eV. For the estimation of BTPTT-4F optical bang gap, we have employed different theoretical methods whose results are reported in Table 1.

Taking into account that Fan et al. [17] report an optical band gap of about 1.7 eV of BTPTT-4F solution in chlorobenzene, DFT calculations with BP functional and ZINDO/S calculations give optical band gaps that are closer to the experimental one.

We perform Hückel method based calculations with Hulis package [34,35]. We find the following states: i) HOMO-1: $\alpha + 0.42\beta$; ii) HOMO: $\alpha + 0.24\beta$; iii) LUMO: $\alpha - 0.15\beta$; iv) LUMO + 1: $\alpha - 0.16\beta$. Hence, we observe a HOMO-LUMO gap of 0.39β. As reported by Fan et al. [17], the experimental HOMO, measured by cyclic voltammetry, is at −5.68 eV, while the experimental LUMO is at −4.06 eV. Thus, we could estimate a value of 4.15 for the β parameter.

Conclusion

In this work, we have studied the optical properties of five different non-fullerene acceptors by means of different calculation methods. These molecules, namely Cz-RH, Flu-RH, TPDI-Hex, IT-4F and BTPTT-4F, hold great promises for application in organic photovoltaic. In regards of BTPTT-4F, which has shown remarkable photovoltaic performances in organic heterojunction cells, we have determined the optical gap and compared it with the experimental results. At this stage, we did not consider any solvent effect on our calculations. However, we propose to include this degree of complexity in the near future, as solvent effects can lead to diverse intramolecular phenomena that, in turns, can modify the optical response of many molecular systems [41].

CRediT authorship contribution statement

Andrea Farina: Data curation. **Giuseppe M. Paternò:** Formal analysis. **Francesco Scotognella:** Conceptualization, Data curation, Formal analysis, Supervision.

Declaration of Competing Interest

The authors declare that they have no known competing financial interests or personal relationships that could have appeared to influence the work reported in this paper.

Acknowledgement

References

[1] He Y, Li Y. Fullerene derivative acceptors for high performance polymer solar cells. Phys Chem Chem Phys 2011;13:1970–83. https://doi.org/10.1039/C0CP01178A.

[2] Sariciftci NS, Smilowitz L, Heeger AJ, Wudl F. Photoinduced electron transfer from a conducting polymer to buckminsterfullerene. Science 1992;258:1474–6. https://doi.org/10.1126/science.258.5087.1474.

[3] Dennler G, Scharber MC, Brabec CJ. Polymer-fullerene bulk-heterojunction solar cells. Adv Mater 2009;21:1323–38. https://doi.org/10.1002/adma.200801283.

[4] Nelson J. Polymer:fullerene bulk heterojunction solar cells. Mater Today 2011;14: 462–70. https://doi.org/10.1016/S1369-7021(11)70210-3.

[5] Paternó G, Warren AJ, Spencer J, Evans G, García Sakai V, Blumberger J, et al. Micro-focused X-ray diffraction characterization of high-quality [6,6]-phenyl-C 61 -butyric acid methyl ester single crystals without solvent impurities. J Mater Chem C 2013;1:5619–23. https://doi.org/10.1039/C3TC31075B.

[6] Paternó G, Cacialli F, García-Sakai V. Structural and dynamical characterization of P3HT/PCBM blends. Chem Phys 2013;427:142–6. https://doi.org/10.1016/j.chemphys.2013.10.006.

[7] Tregnago G, Wykes M, Paternò GM, Beljonne D, Cacialli F. Low-temperature photoluminescence spectroscopy of solvent-free PCBM single-crystals. J Phys Chem C 2015;119:11846–51. https://doi.org/10.1021/acs.jpcc.5b02345.

[8] Lazzerini GM, Paternò GM, Tregnago G, Treat N, Stingelin N, Yacoot A, et al. Traceable atomic force microscopy of high-quality solvent-free crystals of [6,6]-phenyl-C61-butyric acid methyl ester. Appl Phys Lett 2016;108:053303. https://doi.org/10.1063/1.4941227.

[9] Paternò GM, Skoda MWA, Dalgliesh R, Cacialli F, Sakai VG. Tuning fullerene intercalation in a poly (thiophene) derivative by controlling the polymer degree of self-organisation. Sci Rep 2016;6:34609. https://doi.org/10.1038/srep34609.

[10] Lee HKH, Telford AM, Röhr JA, Wyatt MF, Rice B, Wu J, et al. The role of fullerenes in the environmental stability of polymer:fullerene solar cells. Energy Environ Sci 2018;11:417–28. https://doi.org/10.1039/C7EE02983G.

[11] Wadsworth A, Moser M, Marks A, Little MS, Gasparini N, Brabec CJ, et al. Critical review of the molecular design progress in non-fullerene electron acceptors towards commercially viable organic solar cells. Chem Soc Rev 2019;48:1596–625. https://doi.org/10.1039/C7CS00892A.

[12] Sun H, Song X, Xie J, Sun P, Gu P, Liu C, et al. PDI derivative through fine-tuning the molecular structure for fullerene-free organic solar cells. ACS Appl Mater Interfaces 2017;9:29924–31. https://doi.org/10.1021/acsami.7b08282.

[13] Fan X, Gao J, Wang W, Xiao S, Zhan C, Lu X, et al. Ladder-type nonacyclic arene bis (thieno[3,2-b]thieno)cyclopentafluorene as a promising building block for non-fullerene acceptors. Chem Asian J 2019;14:1814–22. https://doi.org/10.1002/asia.201801669.

[14] Chen W, Zhang Q. Recent progress in non-fullerene small molecule acceptors in organic solar cells (OSCs). J Mater Chem C 2017;5:1275–302. https://doi.org/10.1039/C6TC05066B.

[15] Gurney RS, Lidzey DG, Wang T. A review of non-fullerene polymer solar cells: from device physics to morphology control. Rep Prog Phys 2019;82:036601. https://doi.org/10.1088/1361-6633/ab0530.

[16] Duan L, Elumalai NK, Zhang Y, Uddin A. Progress in non-fullerene acceptor based organic solar cells. Sol Energy Mater Sol Cells 2019;193:22–65. https://doi.org/10.1016/j.solmat.2018.12.033.

[17] Fan B, Zhang D, Li M, Zhong W, Zeng Z, Ying L, et al. Achieving over 16% efficiency for single-junction organic solar cells. Sci China Chem 2019;62:746–52. https://doi.org/10.1007/s11426-019-9457-5.

[18] Yuan J, Zhang Y, Zhou L, Zhang G, Yip H-L, Lau T-K, et al. Single-junction organic solar cell with over 15% efficiency using fused-ring acceptor with electron-deficient core. Joule 2019;3:1140–51. https://doi.org/10.1016/j.joule.2019.01.004.

[19] Yan T, Song W, Huang J, Peng R, Huang L, Ge Z. 16.67% Rigid and 14.06% flexible organic solar cells enabled by ternary heterojunction strategy. Adv Mater 2019;31: 1902210. https://doi.org/10.1002/adma.201902210.

[20] Kymakis E, Amaratunga GAJ. Carbon nanotubes as electron acceptors in polymeric photovoltaics. Rev Adv Mater Sci 2005;10:300–5.

[21] Ferguson AJ, Blackburn JL, Kopidakis N. Fullerenes and carbon nanotubes as acceptor materials in organic photovoltaics. Mater Lett 2013;90:115–25. https://doi.org/10.1016/j.matlet.2012.08.145.

[22] Soavi G, Scotognella F, Viola D, Hefner T, Hertel T, Cerullo G, et al. High energetic excitons in carbon nanotubes directly probe charge-carriers. Sci Rep 2015;5:1–5. https://doi.org/10.1038/srep09681.

[23] Hanwell MD, Curtis DE, Lonie DC, Vandermeersch T, Zurek E, Hutchison GR. Avogadro: an advanced semantic chemical editor, visualization, and analysis platform. J Cheminf 2012;4:17. https://doi.org/10.1186/1758-2946-4-17.

[24] Neese F. The ORCA program system. Wiley Interdiscipl Rev Comput Mol Sci 2012; 2:73–8. https://doi.org/10.1002/wcms.81.

[25] Lee C, Yang W, Parr RG. Development of the Colle-Salvetti correlation-energy formula into a functional of the electron density. Phys Rev B 1988;37:785–9. https://doi.org/10.1103/PhysRevB.37.785.

[26] Schäfer A, Horn H, Ahlrichs R. Fully optimized contracted Gaussian basis sets for atoms Li to Kr. J Chem Phys 1992;97:2571–7. https://doi.org/10.1063/1.463096.

[27] Schäfer A, Huber C, Ahlrichs R. Fully optimized contracted Gaussian basis sets of triple zeta valence quality for atoms Li to Kr. J Chem Phys 1994;100:5829–35. https://doi.org/10.1063/1.467146.

[28] Eichkorn K, Weigend F, Treutler O, Ahlrichs R. Auxiliary basis sets for main row atoms and transition metals and their use to approximate Coulomb potentials. Theor Chem Accounts Theory Comput Model (Theor Chim Acta) 1997;97:119–24. https://doi.org/10.1007/s002140050244.

[29] E.~F.~Valeev, A library for the evaluation of molecular integrals of many-body operators over Gaussian functions, (2014). http://libint.valeyev.net/.

[30] Lehtola S, Steigemann C, Oliveira MJT, Marques MAL. Recent developments in libxc — A comprehensive library of functionals for density functional theory. SoftwareX 2018;7:1–5. https://doi.org/10.1016/j.softx.2017.11.002.

[31] Marques MAL, Oliveira MJT, Burnus T. Libxc: a library of exchange and correlation functionals for density functional theory. Comput Phys Commun 2012;183: 2272–81. https://doi.org/10.1016/j.cpc.2012.05.007.

[32] Weigend F, Ahlrichs R. Balanced basis sets of split valence, triple zeta valence and quadruple zeta valence quality for H to Rn: design and assessment of accuracy. Phys Chem Chem Phys 2005;7:3297–305. https://doi.org/10.1039/B508541A.

[33] Weigend F. Accurate coulomb-fitting basis sets for H to Rn. Phys Chem Chem Phys 2006;8:1057–65. https://doi.org/10.1039/B515623H.

[34] Carisson Y, Hagebaum-Reignier D, Goudard N, Humbel S. Hückel-lewis projection method: a "weights watcher" for mesomeric structures. J Phys Chem A 2008;112: 13256–62. https://doi.org/10.1021/jp803813e.

[35] Huckel Theory and HuLiS: a calculator that also describes mesomerism., (2013). http://www.hulis.free.fr/ (accessed June 8, 2020).

[36] Kim Y, Song CE, Moon S-J, Lim E. Effect of dye end groups in non-fullerene fluorene- and carbazole-based small molecule acceptors on photovoltaic performance. RSC Adv 2015;5:62739–46. https://doi.org/10.1039/C5RA03607K.

[37] Kim Y, Song CE, Moon S-J, Lim E. Rhodanine dye-based small molecule acceptors for organic photovoltaic cells. Chem Commun 2014;50:8235–8. https://doi.org/10.1039/C4CC01695E.

[38] Hendsbee AD, Sun J-P, Law WK, Yan H, Hill IG, Spasyuk DM, et al. Synthesis, self-assembly, and solar cell performance of n-annulated perylene diimide non-fullerene acceptors. Chem Mater 2016;28:7098–109. https://doi.org/10.1021/acs.chemmater.6b03292.

[39] Li S, Ye L, Zhao W, Zhang S, Mukherjee S, Ade H, et al. Energy-level modulation of small-molecule electron acceptors to achieve over 12% efficiency in polymer solar cells. Adv Mater 2016;28:9423–9. https://doi.org/10.1002/adma.201602776.

[40] Zhao W, Li S, Yao H, Zhang S, Zhang Y, Yang B, et al. Molecular optimization enables over 13% efficiency in organic solar cells. J Am Chem Soc 2017;139: 7148–51. https://doi.org/10.1021/jacs.7b02677.

[41] Marini A, Muñoz-Losa A, Biancardi A, Mennucci B. What is solvatochromism? J Phys Chem B 2010;114:17128–35. https://doi.org/10.1021/jp1097487.